Molecular-Dynamics Simulation of Wetting and Drying at Solid-Fluid Interfaces

J. H. Sikkenk, J. O. Indekeu,[a] and J. M. J. van Leeuwen
Instituut Lorentz, Rijksuniversiteit te Leiden, NL-2311 SB Leiden, The Netherlands

and

E. O. Vossnack
Laboratorium voor Technische Natuurkunde, Technische Universiteit Delft, NL-2600GA Delft, The Netherlands
(Received 6 April 1987)

Computer simulations of a Lennard-Jones fluid adsorbed at a structured solid substrate have been carried out with the Delft Molecular Dynamics Processor, using about 11 500 particles. Realistic density profiles have been obtained. By measurement of surface tensions and contact angles, a wetting as well as a drying phase transition have been identified. The wetting transition had not previously been seen in computer simulations of continuum fluids. Both transitions are of first order.

PACS numbers: 68.45.Gd, 61.20.Ja, 68.10.Cr, 82.65.Dp

Simulations of a Lennard-Jones fluid in contact with a wall can complement theoretical and experimental studies of wetting phenomena. The main issues are the existence and the nature of a wetting or drying phase transition. This transition is expected at the solid-fluid interface at liquid-vapor coexistence, when the temperature is increased towards the critical temperature of the fluid.[1-5] In the case of a wetting transition an adsorbed liquid film of *microscopic* thickness grows suddenly into a layer of *macroscopic* thickness. At a drying transition the adsorbed phase is a vapor. Computer simulations of the wetting or drying transitions are difficult because one needs a large system to accommodate the various phases, and consequently the system equilibrates slowly near the transitions. Previous simulation studies of adsorption dealt with numbers of particles ranging between 200 and 1200, and represented the influence of walls by external potentials[6,7] which are independent of the transverse coordinates and thereby leave out corrugation effects.

The wetting transition has not previously been observed in computer simulations. A *drying* phase transition has been reported. van Swol and Henderson[6] located a drying transition in a system of 512 particles interacting through square-well potentials on the basis of examination of density profiles and coverages in addition to an analysis of surface tension data, with the help of statistical sum rules. In their system it is not possible to observe a wetting phase transition.

We report on simulations using the Delft Molecular Dynamics Processor[8] with two types of particles, 2904 of one type for building a solid substrate and about 8500 of the other type for composing the fluid adsorbate. All particles interact through Lennard-Jones potentials. Consequently, the fluid is in contact with a live wall. As an important advantage, all interfacial tensions are measurable as mechanical forces rather than being obtained indirectly from surface free energies. We obtain *realistic* density profiles and capture *both* phase transitions.

The condition of thermodynamic stability

$$\gamma_{SV} \leq \gamma_{SL} + \gamma_{LV} \tag{1a}$$

expresses that a solid-vapor interface with surface tension γ_{SV} will be thermodynamically stable as long as the inequality is strictly satisfied. In this case the solid is incompletely wetted. If the equality is realized, the stable profile consists of a solid-liquid interface with tension γ_{SL} combined with a liquid-vapor interface with tension γ_{LV} far away. The solid is then completely wetted. Analogously,

$$\gamma_{SL} \leq \gamma_{SV} + \gamma_{LV} \tag{1b}$$

expresses (in)complete drying of the solid. For incomplete wetting or drying, the contact angle Θ is defined by

$$\gamma_{LV}\cos\Theta \equiv \gamma_{SV} - \gamma_{SL}, \tag{2}$$

expressing mechanical equilibrium of a three-phase contact line.

Our system can support solid-liquid, solid-vapor, and liquid-vapor interfaces. Bulk liquid-vapor coexistence is enforced by the presence of at least one free liquid-vapor interface. *Symmetric* profiles consist of two solid-liquid (or two solid-vapor) interfaces and two liquid-vapor interfaces bounding a vapor (or liquid) phase in the middle (Fig. 1). An *asymmetric* profile consists of one solid-vapor, one solid-liquid, and one liquid-vapor interface (Fig. 2). The symmetric profiles correspond to a total surface tension $2\gamma_{SL}+2\gamma_{LV}$ (or $2\gamma_{SV}+2\gamma_{LV}$), whereas the asymmetric profile has $\gamma_{SL}+\gamma_{SV}+\gamma_{LV}$.

For studying wetting, instead of varying the temperature, we vary the relative strength of the solid-fluid and the fluid-fluid interactions. This is generally referred to as varying the "surface field,"[9] which in our system is

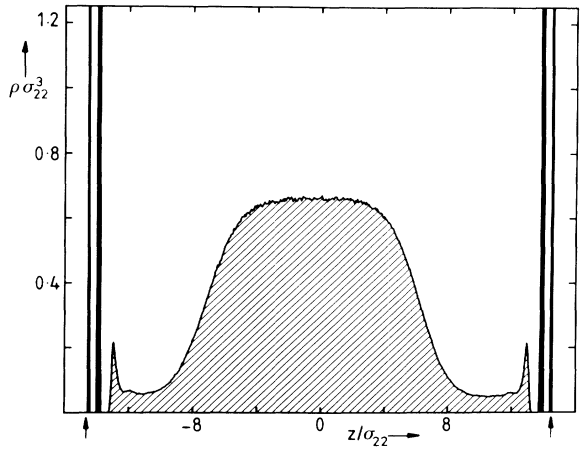

FIG. 1. Symmetric density profile at $\epsilon_r=0.3$ after a trajectory of 2.6×10^4 time steps after equilibration. The dark peaks correspond to the substrate layers and the shaded area to the fluid. The arrows denote the periodic boundary.

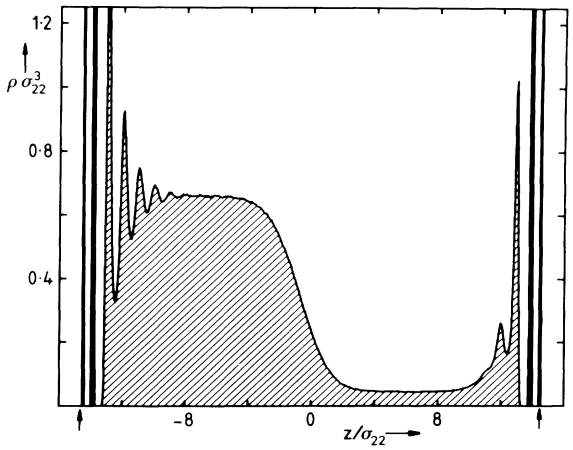

FIG. 2. Asymmetric density profile at $\epsilon_r=0.65$ after a trajectory of 5.2×10^4 time steps after equilibration.

represented by the ratio $\epsilon_r=\epsilon_{12}/\epsilon_{22}$ of the Lennard-Jones parameters, where 1 refers to particles in the wall and 2 to particles in the fluid.

At constant temperature, depending on ϵ_r, the thermodynamically stable profile, which minimizes the total surface tension $\gamma_{\rm tot}$, can have various symmetries. If wetting or drying phase transitions take place, singularities occur in the minimal total surface tension as a function of ϵ_r. In the case of a first-order transition the derivative of $\gamma_{\rm tot}$ is discontinuous and metastable continuations of stable-profile symmetries are expected.

We have computed $\gamma_{\rm tot}$ from integrating the difference of normal and transverse pressure-tensor components across the system[10]:

$$\gamma_{\rm tot}=\int_{-L/2}^{L/2}dz\,[p_N(z)-p_T(z)], \tag{3}$$

where L is the linear size of our cubic box and z measures the distance perpendicular to the substrate. Alternatively, we have divided $\gamma_{\rm tot}$ into the contributions corresponding to the different interfaces and checked explicitly Eqs. (1) and (2), thus obtaining contact angles.

The speed of the special-purpose computer which we have used is comparable to that of a Cray-1 supercomputer. Our simulations took a total of about 2000 hours of central-processing-unit time. The Lennard-Jones potential parameters are ϵ_{22} and σ_{22} for the fluid particles. In the solid, $\epsilon_{11}=50\epsilon_{22}$ in order to build a stable close-packed fcc solid substrate of three layers. The lattice spacing, dictated by $\sigma_{11}=0.847\sigma_{22}$, is chosen such that there is a mismatch between solid and fluid to prevent solidification of the first adsorbed liquid layers. Particles in the solid are three times more massive than in the fluid ($m_1=3m_2$). As a consequence, apart from small vibrations the substrate is rigid. The interaction between substrate and adsorbate particles is characterized by ϵ_{12} and $\sigma_{12}=0.912\sigma_{22}$. All pair potentials are cut off at 2.5σ. The temperature of our simulations equals $T^*=k_BT/\epsilon_{22}=0.9$, which is between the triple and the critical temperatures of the bulk fluid. The temperature is kept constant by regular adjustment of the kinetic energy. The linear box size L is $29.1\sigma_{22}$ and the boundary conditions are periodic in all three dimensions. The initial configuration for a specific value of ϵ_r was taken to be an equilibrated configuration at a slightly different ϵ_r. We have allowed 1×10^4 time steps of

$$\Delta t^*=t/\sigma_{22}(m_2/\epsilon_{22})^{1/2}=0.01$$

for equilibration. This was sufficient to obtain stable bulk densities, total energy, and coverages in most of the cases. After equilibration, measurements were made of pressure-tensor components, density profile (every thirteen time steps), kinetic energy, potential energy, and pressure (every time step). To get a notion of statistical reliability the runs were divided into subruns of 5200 time steps. Typically runs took from five up to twenty subruns. Error bars in our figures are based on results from these subruns.

At the first stage of our investigation we have looked at density profiles and coverages between $\epsilon_r\simeq0.1$ and $\epsilon_r\simeq1.0$. The following qualitative picture results. At low ϵ_r symmetric (completely dry) profiles occur, and symmetric (completely wet) profiles are seen at high ϵ_r. In between, asymmetric profiles appear. There are large overlaps where both symmetries are found.

Second, we addressed the question of the total surface free energy of a configuration as defined in Eq. (3). Figure 3 displays $\gamma_{\rm tot}$ vs ϵ_r. Data points with open circles refer to asymmetric profiles. Filled squares and circles correspond to symmetric profiles. We distinguish three curves. First, there is a curve between $\epsilon_r\simeq0.1$ and $\epsilon_r\simeq0.8$, which is more or less a straight line, associated with asymmetric profiles. This curve meets a steep curve

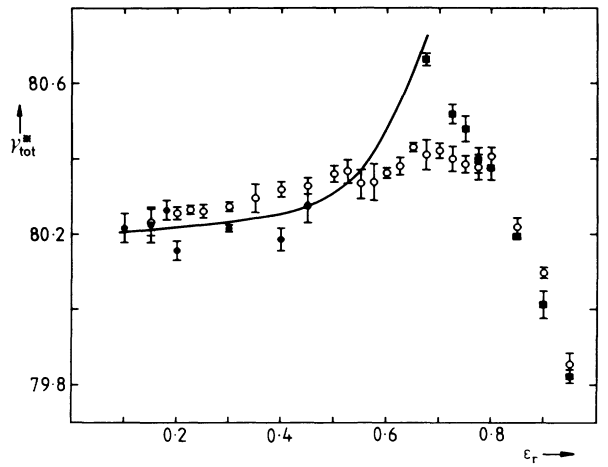

FIG. 3. The total surface tension γ_{tot} in units of $\epsilon_{22}/\sigma_{22}^2$ vs ϵ_r. Open circles correspond to asymmetric profiles and filled circles and squares to symmetric profiles. The full curve is obtained from contact-angle measurements (Fig. 4).

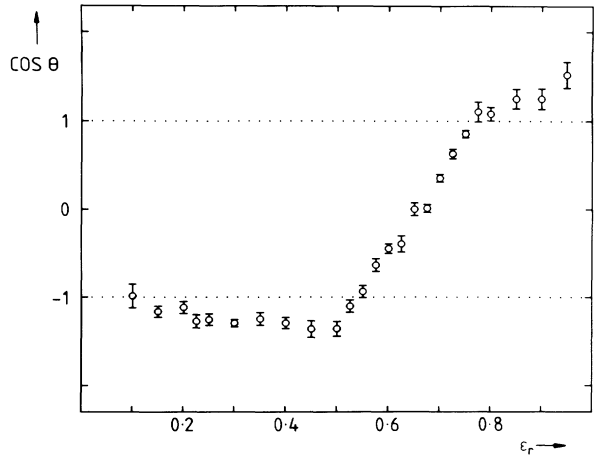

FIG. 4. The cosine of the contact angle Θ vs ϵ_r for asymmetric profiles.

(squares) representing completely wetted substrates at $\epsilon_r \simeq 0.8$, and almost merges with the latter at higher ϵ_r. We see that below $\epsilon_r = 0.78 \pm 0.03$ the incompletely wetted substrate is the thermodynamically more stable configuration, whereas the completely wetted substrate minimizes γ_{tot} above this value of ϵ_r. The third curve (filled circles) consists of data points of completely dry substrates. These data are based on relatively short observation times (about four subruns) and therefore are less accurate. However, if the data are complemented with information from contact-angle measurements, the drawn curve results for the total surface tension of completely dry substrates. We see that below $\epsilon_r = 0.54 \pm 0.03$ the completely dry substrate minimizes γ_{tot}, whereas the incompletely dry substrate is the thermodynamically more stable configuration at higher ϵ_r.

Third, we measured contact angles on the basis of surface tensions corresponding to the distinct interfaces in the system. This is easy whenever interfaces are separated by bulk phases where the integrand of (3) vanishes. We have obtained $\gamma_{LV} = 0.22 \pm 0.01$ and found that it is independent of ϵ_r. Less obvious is the identification of γ_{SL} and γ_{SV}, because the solid substrate is only three atomic layers thick. We have obtained an approximate separation between the two tensions as follows. Contributions to the integrand in Eq. (3) arising from the interaction of the substrate with the adsorbate on one side have been attributed to the interfacial tension on that side. Figure 4 shows $\cos\Theta$, as obtained from Eq. (2), for asymmetric profiles (open circles in Fig. 3). The data corresponding to *incompletely* dry or wetted substrates ($-1 < \cos\Theta < 1$) follow a strikingly straight line. These data suggest that incompletely wetted substrates are metastable for $\epsilon_r \gtrsim 0.78$ and that incompletely dry substrates are metastable for $\epsilon_r \lesssim 0.54$. This is so because these states violate Eqs. (1).

We now comment on the shorter observation times of completely dry substrates at liquid-vapor coexistence. The position of the center of mass of a liquid droplet as in Fig. 1 fluctuates in time because of velocity fluctuations inherent in our simulations. Independently of ϵ_r this causes the substrate and the droplet to collide, typically after four subruns. At very low ϵ_r (e.g., at 0.1) this hardly damages the droplet, and the droplet leaves the wall after a considerable time (fifteen subruns). At ϵ_r around 0.4 the collision changes the profile drastically and the illusion of a phase transition to the incompletely dry substrate is created. Indeed, a latent heat of adsorption of order 1 (in units of $\epsilon_{22}/\sigma_{22}^2$) is absorbed by the heat bath. As can be seen in Fig. 3 γ_{tot} is *increased* by an amount of order 0.1, and thus a *metastable* state is reached.[11] The time that the droplet stays at the wall is longer than we are able to measure.

On the basis of all our data, we conclude that there is a first-order wetting transition at $\epsilon_r \simeq 0.78$ and a first-order drying transition at $\epsilon_r \simeq 0.54$. The discontinuity in slope of γ_{tot} (deduced from the contact-angle data in Fig. 4) is approximately the same for both.

Our present study has been complicated by interferences between different interfaces in some cases. This can only be remedied by simulation in a box which is much longer in the z direction than in the transverse directions. Future studies should include effects of the long-range tails of the van der Waals forces and a search for the prewetting phenomenon.

We are very grateful to Dr. A. F. Bakker for making available for our simulations the special-purpose computer Delft Molecular Dynamics Processor developed by him. We have enjoyed stimulating discussions with Dr. C. Bruin, Dr. D. Frenkel, M. Nijmeijer, and Professor W. Van Dael, and received extensive and inspiring correspondence from Professor J. Henderson. Part of

this research was supported by the Stichting voor Fundamenteel Onderzoek der Materie, which is financially supported by the Nederlandse Organisatie voor Zuiver-Wetenschappelijk Onderzoek. One of us (J.O.I.) acknowledges support from the Belgian National Fund for Scientific Research.

[a]Present address: Molecular Physics Laboratory, Katholieke Universiteit Leuven, B-3030 Leuven, Belgium.

[1]J. W. Cahn, J. Chem. Phys. **66**, 3667 (1977).

[2]C. Ebner and W. F. Saam, Phys. Rev. Lett. **38**, 1486 (1977).

[3]D. E. Sullivan, Phys. Rev. B **20**, 3991 (1979), and J. Chem. Phys. **74**, 2604 (1981).

[4]P.-G. de Gennes, Rev. Mod. Phys. **57**, 827 (1985).

[5]M. R. Moldover and J. W. Schmidt, Physica (Amsterdam) D **12**, 351 (1984).

[6]F. van Swol and J. R. Henderson, J. Chem. Soc. Faraday Trans. 2 **82**, 1685 (1986).

[7]G. Saville, J. Chem. Soc. Faraday Trans. 2 **73**, 1122 (1977).

[8]A. F. Bakker, in *Materials Research Society Symposia Proceedings Vol. 63,* edited by J. Broughton, W. Krakow, and S. T. Pantelides (Materials Research Society, Pittsburgh, PA, 1986), p. 181; H. J. Hilhorst, A. F. Bakker, C. Bruin, A. Compagner, and A. Hoogland, J. Stat. Phys. **34**, 987 (1984).

[9]H. Nakanishi and M. E. Fisher, Phys. Rev. Lett. **49**, 1565 (1982).

[10]J. S. Rowlinson and B. Widom, *Molecular Theory of Capillarity* (Oxford Univ. Press, New York, 1982).

[11]This is true to the extent that the bulk contributions to the total free energy are not affected.